Journal of Applied Polymer Science

Process-structure-property relationship of melt spun poly(lactic acid) fibers produced in the spunbond process

Eunkyoung Shim, Behnam Pourdeyhimi, Don Shiffler
1020 Main Campus Drive, North Carolina State University, Raleigh, North Carolina 27695-8301
Correspondence to: E. Shim (E-mail: eshim@ncsu.edu)

ABSTRACT: We report on the process–structure–property relationships for Poly(lactic acid) (PLA) filaments produced through the spunbond process. The influence of spinning speed, polymer throughput, and draw ratio on crystallinity and birefringence of fibers were evaluated. We established that increasing spinning speed increases crystallinity and birefringence of fibers. We also investigate the role of fiber structures on fiber tensile properties—breaking tensile strength, strain at break, initial modulus, and natural draw ratio. An increase in spinning speed leads to a higher breaking tensile strength, higher initial modulus and lower strain at break. We have shown an almost linear relationship between breaking tensile strength of PLA fibers and birefringence. This indicates that improved tensile properties at high spinning speeds can be attributed to enhanced molecular orientation. The dependency of fiber breaking tensile strength and strain at break on spun orientation were explained with natural draw ratio, as a measure of spun orientation. © 2016 Wiley Periodicals, Inc. J. Appl. Polym. Sci. **2016**, *133*, 44225.

KEYWORDS: fibers; polyesters; structure-property relations; textiles

Received 10 June 2016; accepted 16 July 2016
DOI: 10.1002/app.44225

INTRODUCTION

Increasing concerns over sustainable development and environmental protection have generated pressure and interests in the use and development of polymers produced from renewable resources. One of most well-known polymers produced from renewable resources is Poly(lactic acid) (PLA). PLA is an aliphatic polyester that can be prepared by both direct condensation of lactic acid and by the ring-opening polymerization of the cyclic lactide dimer. Lactic acid, the starting materials of both processes, is made by a fermentation process using 100% annually renewable resources such as wheat, sugar canes, corn, and etc.[1,2] PLA is also known for its compostablity as it rapidly degrades in the environment and is converted to low toxicity products including carbon dioxide and water.[2–4]

Because PLA is thermoplastic and can be processed through various melt processing,[5] it has been recognized as one prominent alternative for the replacement of conventional petroleum-derived polymers. Since it was introduced as a commercially available material produced from renewable resources, the volume of PLA polymer production continues to grow and applications of it are also widened.[6] It has been introduced wide ranges of applications including medical/pharmaceutical, packaging, and housewares.[7]

As PLA is melt-spinnable,[8] it has been used for producing fibers and PLA fibers have been used in fiberfill, apparel, geotextiles, hygiene products, wipes, and fiber-based composites.[7] Compared to films, nonwovens and textiles are known to provide many beneficial characteristics because of their high surface area. Several studies have reported formation of PLA fibers via melt spinning,[9–14] wet or dry solution spinning,[15–18] and electrospinning process.[19–21] Among those various fiber formation processes, melt spinning is the most economical process and the most preferred spinning technique in textiles and nonwovens industry. As it does not use any solvent or chemicals for coagulations of polymer, melt spinning is environmentally friendly fiber formation process. One of the reasons PLA polymer has been received the most attention among polymers derived from renewable resources is its melt processiblity. The attempt to produce PLA fibers via melt spinning can be traced back to 1970s.[22] For the last two decades, melt spinning of PLA has been studied by many researchers. Most early studies have been conducted at very low collection speed, less than <20 m/min, which is the order of magnitude lower than industrial scale melt spinning.[9] These may not translate to high speed, as melt spinning is a complex process in which, the fiber fine structure development is determined by the manner in which the polymer responds to tension, temperature, and shear deformation in the spin-line. It is known that spinning speed plays important role in the development of fiber structure during melt spinning and fiber properties.[14,23,24] Several research reported high speed melt spinning of PLA filaments.[10,12,13] These confirm that

Table I. Spinning Conditions of PLA Fibers Produced with the Spunbond System

Sample ID	Throughput, Q (g hole^{-1} min^{-1})	Spinning speed, S (m min^{-1})	Fiber diameter (μm)
SB 0.4-1	0.4	1024	19.9 ± 1.4
SB 0.4-2	0.4	2330	13.2 ±0.9
SB 0.4-3	0.4	3090	11.5 ± 1.4
SB 0.4-4	0.4	3228	11.2 ± 1.3
SB 0.4-5	0.4	3836	10.3 ± 1.3
SB 0.7-1	0.7	697	32.0 ± 2.6
SB 0.7-2	0.7	1154	24.9 ± 1.9
SB 0.7-3	0.7	2520	16.8 ± 1.1
SB 0.7-4	0.7	3047	15.3 ± 0.8
SB 0.7-5	0.7	3318	14.7 ± 1.1
SB 0.7-6	0.7	3586	14.1 ± 1.1
SB 1.0-1	1.0	1158	29.5 ± 2.6
SB 1.0-2	1.0	1871	23.2 ± 1.7
SB 1.0-3	1.0	2489	20.1 ± 1.0
SB 1.0-4	1.0	3186	17.8 ± 1.3
SB 1.0-5	1.0	3236	17.7 ± 0.8

significant influences of spinning conditions—including spinning speed on molecular structure of PLA fibers and their properties.

The spunbond process, one of most used nonwoven manufacturing technology, shares fundamental principles of fiber melt spinning process. It involves direct conversion of a polymer into nonwovens consisting of randomly laid continuous filaments. Thus, the spunbond technology combines fiber spinning and fabric formation to a single process with high production speed. So the spunbond process is one of the most economical technology to convert polymers to fabrics. Spunbond nonwovens are widely used in variety of different applications including carpet backings, medical, and filtration applications.[25] Large portion of spunbond nonwoven products are disposable applications such as diapers and wipes. PLA, with its compostability, is an attractive material in the spunbond process.[26]

The first step of the spunbond process is fiber formation where polymers are melted, extruded, solidified, and drawn. It is evolved from filament melt spinning process, sharing same principles of fiber formation and the step where microstructure and fiber properties are determined. However, there are differences. Fiber formation in the modern spunbond bonding process is a curtain spinning process, where fibers extruded through a spin beam, which has multiple rows of spinnerets with the spinneret density of 3000–6000 holes/m and 1–5 m width. Then fibers are quenched and drawn by high speed air. Fibers produced will be collected with a web lay down system, such as a belt or a drum collector. As drawing and collection of fibers on the belt are carried out by processing air, so spinning speed is controlled by processing air pressure and the equipment configuration. In contrast, traditional textile melt filament spinning process which produces filaments or staples fibers is two-step process consisting of melt extrusion and drawing. Polymer melts are extruded through spinnerets, quenched, and collected by the winder. The spinning speed or collection speed of fibers produced will be controlled by the winder rotating speed. So more precise control of the spinning speed can be achieved in the melt spinning. Fibers will be drawn to achieve increasing orientation and crystallinity and to improve their mechanical properties.[27,28] Drawing of typical filament/staple fiber is often carried out after spinning by using series of winders and temperatures and speed of these winders can be controlled separately. So, more precise controls of draw ratio can be achieved.

Even filament spinning of PLA has been reported in the literature, little can be found in fiber formation of PLA fibers in spunbond technology. So, PLA fiber formation process during the spunbond process is worth to study. Since properties of polymeric fibers are highly influenced by the microstructure of the resultant fiber, it is essential to establish the manner in which process variable influence process–structure–properties in PLA fibers. Below, we report on the evolution of the morphology in PLA fiber produced from a commercially available fiber grade PLA resin and its influence on tensile properties.

EXPERIMENTAL

Sample Production

Fiber grade Poly(lactic acid) (PLA) resin supplied by NatureWorks® (Polymer 6202D) with a melt flow index of 15–30 g/10 min (at 210 °C), specific gravity of 1.24 and D-lactide content of 2% was used to produce fibers.

PLA fibers were produced with Nordson Fiber/Hills. Bicomponent spunbonding system in the Nonwovens Institute Partner's lab located at North Carolina State University (Raleigh, NC). The temperature profile of the 6-zone extruder used was 204 °C–221 °C–226 °C–232 °C–238 °C–238 °C from zone 1 to zone 6, respectively. The diameter of the spinneret used was 0.35 mm. Detailed description of process and the fibers produced are shown in Table I. Fiber diameters given in Table I were measured microscopically with a Nikon SMZ1000 stereozoom microscope and spinning speeds are controlled by process air pressure in the aspirator and calculated from polymer throughput and fiber diameter.[29]

Differential Scanning Calorimetry

The thermal transitions of PLA fibers were investigated using Differential Scanning Calorimetry (DSC) (Perkin Elmer Diamond DSC). The DSC was calibrated using the melting temperature and enthalpy of indium. The samples with a weight ranging from 3 to 5 mg were sealed into an aluminum pan and heated from 20 °C to 250 °C at the rate of 20 °C min^{-1}.

Crystallinity was calculated using the following formula:

$$X_c = \frac{H_f - H_c}{93} \quad (1)$$

where H_f and H_c are the enthalpies of fusion and crystallization, respectively, and 93 J g^{-1} is the enthalpy of fusion of PLA crystals.[30]

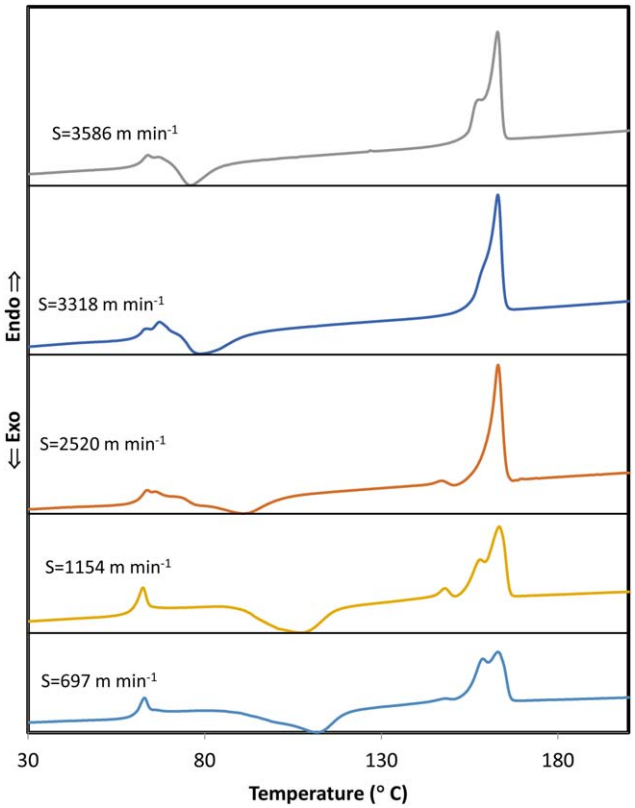

Figure 1. DSC melting thermograms of PLA fibers. Throughput = 0.7 g hole^{-1} m^{-1}. [Color figure can be viewed in the online issue, which is available at wileyonlinelibrary.com.]

Birefringence

Birefringence of PLA fiber samples were measured by the interference fringe shift method with an Aus Jena Mach-Zehnder type interference microscope. Fibers are immersed in the oil with matching refractive index (Cargill) and refractive index of parallel and perpendicular to fiber axis were measured and the difference of values taken as birefringence.

Tensile Properties

Tensile properties of single PLA fibers were assessed with an Instron Universal tensile testing machine according to ASTM D 3822. Breaking strength, stain at break, initial modulus, and natural draw ratio of were obtained from the stress–strain curve. Average and standard error of 10 fibers are reported.

RESULTS AND DISCUSSION

DSC Analysis and Crystallinity

DSC thermograms of PLA fibers reveal a series of thermal transition of melt-spun PLA fibers–glass transition, relaxation, crystallization, and melting (Figure 1). Broad endothermic peaks at the temperature range 60–70 °C were observed in all samples which can be considered as the relaxation of macromolecules. It is believed that relaxation of macromolecules occurs immediately after glass transition temperature (T_g). In literature, glass transition of PLA is reported in ranges of 60–70 °C.[31] Just above T_g, the molecules are in a rubbery state so a nonstable conformations gain mobility to form more stable conformations.[32] Since glass transition and PLA chain relaxation occurs in the similar temperature ranges, it is hard to distinguish these two transitions in our DSC analysis.

In most samples, relaxation endotherm followed by cold crystallization observed at the temperature range 70–90 °C. Cold crystallization temperature and heat of crystallization of fibers are summarized in Figure 2. PLA fibers spun at low spinning speed exhibit broad cold crystallization peak at higher temperature. As the spinning speed increases, the heat of crystallization decreases while on-set crystallization temperature is lowered. It can be explained by the facts that fibers spun at high spinning speed develop more crystalline region and high molecular orientation. Cold crystallization would be most favorable at the region of oriented amorphous region where molecules have some orientation but not yet formed crystalline. As spin speed increases, total orientation of fiber increases, which in turn increases in amorphous orientation. Increasing molecular orientation in amorphous region will reduced crystallization temperature since it requires less molecular mobility. Therefore, high spinning speed results in lowering crystallization temperature. However, the results of increasing amorphous orientation and spin-line tension also cause more crystalline region formation during the

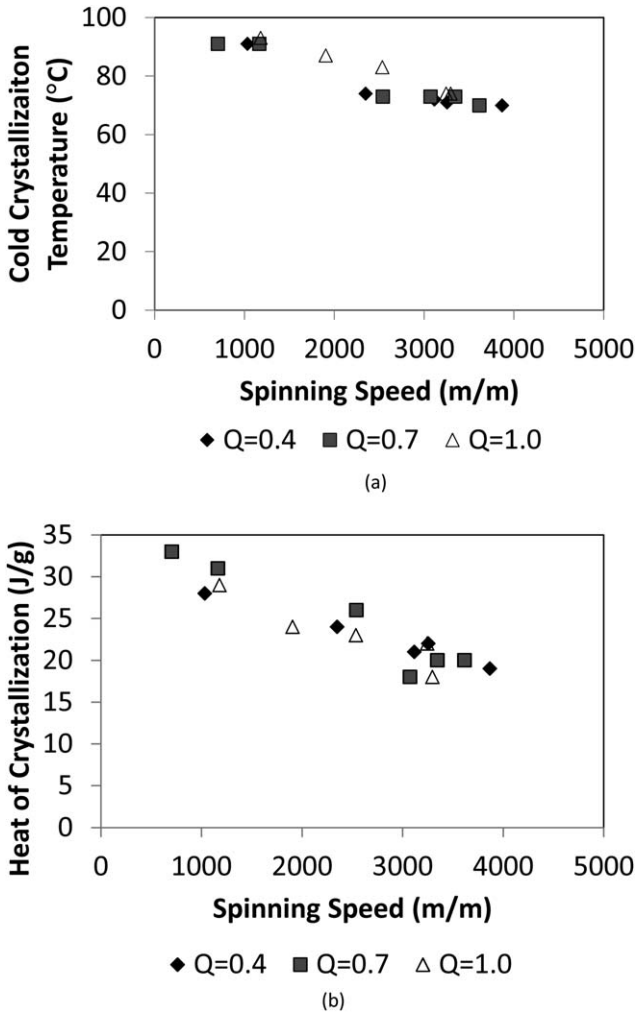

Figure 2. Effects of spinning conditions on cold crystallization behavior of PLA fibers (a) crystallization temperature and (b) Heat of crystallization.

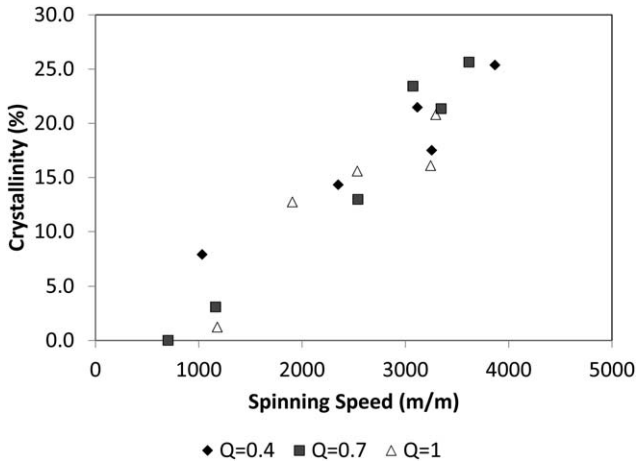

Figure 3. Effects of spinning conditions on crystallinity of PLA fibers.

spinning (shown in Figure 3). So, the amount of cold crystallization occurs will be reduced since reduction of meta-state region. These trends are observed in all samples regardless of throughput.

Melting endotherms were also affected by spinning conditions. Summary of melting temperature of all fibers is given in Table II. PLA fibers spun with low spinning speed showed broad and multiple melting peaks. As the spinning speed increases, melting peaks became larger and shaper. Reduction of satellite peaks was also observed. Some satellite melting peaks may be induced by crystals formed by cold crystallization during the DSC analysis, so disappearance of them may be partly caused by reduction of cold crystallization. However, formation of more perfect and uniform crystal at high spinning speed can be another reason of narrower and sharper melting peaks. Increasing size of melting peak represents increases in the degree of crystallinity at high spinning speed.

Figure 3 shows the effect of spinning speed on crystallinity. As spinning speed increases, crystallinity of sample increases dramatically. Fibers spun under 1000 m/m consist of mostly amorphous region with less than 5% crystallinity while crystallinity of fibers spun at about 4000 m/m spinning speed reaches over 25%.

It can be explained by stress-induced crystallization during fiber melt spinning.[33] PLA has known for its slow crystallization kinetics in quiescent state. At low spinning speed, PLA polymer tends to undergo slow crystallization process and would not have enough time to develop crystalline structure, and forms amorphous state. This changes as spinning speed increases. Increasing spinning speed results in higher spinline tension and stress-induced crystallization would occur. So fibers formed as higher speed have higher crystallinity.

Molecular Orientation

Birefringence of fibers reflects total molecular orientation developed during the fiber formation process. Table III shows birefringence of PLA fibers. Birefringence of fibers increases with spinning speed but decreases as throughput increases. The increase in birefringence is the consequence of improved molecular orientation developed during spinning, which is called spun orientation.

Development of molecular orientation during spinning is governed by spinline tension and crystallization.[12] Tension imparted into spinline would stretch and attenuate the polymer stream and this results in increasing molecular orientation. Bosley[34] discussed fiber molecular orientation in terms of fiber length, where the length of an as-spun fiber is related to the theoretical length that fiber would have if the orientation could be relaxed to zero. Then, the simplest approach to relate molecular orientation development in spinline to spinning parameters is to view molecular orientation as the result of extension of a fiber.

Figure 4 shows a polymer stream in the melt spinning process schematically. A stream of polymer melt exits a spinneret hole at a throughput of Q (g min^{-1}) and it is drawn continuously at a take-up velocity, S (m min^{-1}). The extruded polymer melt initially swells (called die-swell), then is attenuated continuously. In fibers made of organic polymers, orientation of fibers is a function of the total length of the molecules. Assuming that no slippage between molecules occurs, molecular orientation would be directly proportional to the length of the fiber consisting of same amount of polymer. So, spun orientation SO, is the ratio of the length of the given amount of polymer, L to the length of the polymer strand when the polymer chains is relaxed close to zero orientation, L_0. Since the length of polymer stream of the given amount of polymer is proportional to speed, SO, becomes

$$SO = \frac{L}{L_0} \cong \frac{S}{V_0} \tag{2}$$

where S (m min^{-1}) is the take up speed and V_0 is the speed of the polymer stream close to spinneret exit where the polymer

Table II. Melting Temperature (T_m) of PLA Fibers

Throughput = 0.4 g hole^{-1} min^{-1}			Throughput = 0.7 g hole^{-1} min			Throughput = 1.0 g hole^{-1} min		
Sample ID	Spinning speed (m min^{-1})	T_m (°C) (satellite peak)	Sample ID	Spinning speed (m min^{-1})	T_m (°C) (satellite peak)	Sample ID	Spinning speed (m min^{-1})	T_m (°C) (satellite peak)
SB 0.4-1	1033	159 (146)	SB 0.7-1	703	154 (144)	SB 1.0-1	1179	155 (146)
SB 0.4-2	2349	160 (147)	SB 0.7-2	1163	158 (145)	SB 1.0-2	1906	159 (146)
SB 0.4-3	3115	160	SB 0.7-3	2540	160 (147)	SB 1.0-3	2535	160 (145)
SB 0.4-4	3254	159	SB 0.7-4	3072	159	SB 1.0-4	3244	160 (145)
SB 0.4-5	3867	154	SB 0.7-5	3345	159	SB 1.0-5	3295	160 (145)
			SB 0.7-6	3615	159			

Table III. Birefringence of PLA Fibers Produced under Various Spinning Conditions

Throughput = 0.4 g hole^{-1} min^{-1}			Throughput = 0.7 g hole^{-1} min			Throughput = 1.0 g hole^{-1} min		
Sample ID	Spinning speed (m min^{-1})	Birefringence	Sample ID	Spinning speed (m min^{-1})	Birefringence	Sample ID	Spinning speed (m min^{-1})	Birefringence
SB 0.4-1	1033	0.00549	SB 0.7-1	703	0.00194	SB 1.0-1	1179	0.00147
SB 0.4-2	2349	0.01133	SB 0.7-2	1163	0.00382	SB 1.0-2	1906	0.00548
SB 0.4-3	3115	0.01161	SB 0.7-3	2540	0.00865	SB 1.0-3	2535	0.00725
SB 0.4-4	3254	0.01302	SB 0.7-4	3072	0.01222	SB 1.0-4	3244	0.00900
SB 0.4-5	3867	0.01453	SB 0.7-5	3345	0.01055	SB 1.0-5	3295	0.00965
			SB 0.7-6	3615	0.01492			

chains are reflexed. Polymer throughput per hole, Q (g min^{-1}), of the polymer streams at any given point of the spin line becomes

$$Q = \rho A V \tag{3}$$

where ρ is the density of the material, A is the cross-sectional area of the polymer stream, V is the speed.

By conservation of mass, Q would be constant through the spinline, so

$$V_0 = \frac{Q}{\rho A_0} \tag{4}$$

Then, SO becomes

$$SO = \frac{\rho A_0 S}{Q} \propto \frac{S}{Q} \tag{5}$$

where S is the spinning speed of filaments (m min^{-1}), A_0 would be system variable and will be influenced by the equipment used, quench conditions and material used. If these are constant, we can assume A_0 would not change dramatically. Then Spun-orientation for a given system and a given polymer would be linearly proportional to S/Q.

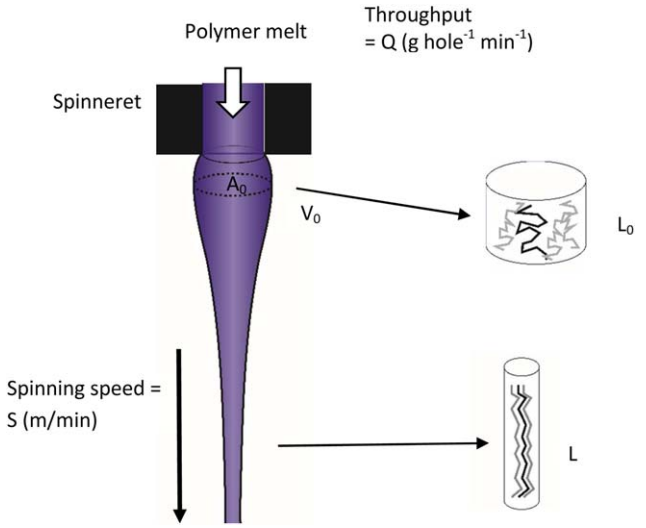

Figure 4. Schematics of spinline and spun-orientation development. The die swell is exaggerated for the purpose of illustration. [Color figure can be viewed in the online issue, which is available at wileyonlinelibrary.com.]

Figure 5 illustrates the effect of spinning speed and throughput on molecular orientation on filaments spun with the spunbond system. Birefringence increases with S/Q, indicating fiber formation mechanism in the spunbond is not drastically different from that in multifilament spinning. For throughput of 0.7 and 1.0 g min^{-1}, linear relationship between S/Q and birefringence were observed as expected in eq. (5). However, fibers spun at 0.4 g min^{-1} behaves differently. Birefringence still more or less increase linearly with S/Q but the slope of the line is lower than fibers with throughput of 0.7 and 1 g min^{-1}. This may be caused by faster solidification as less amount of material need to be cooled down. In addition, decreasing throughput will also reduce shear–stress at the spinneret which may cause reduction of die-swell and A_0.

Fiber Tensile Properties. Typical tensile deformation behaviors of PLA filaments are shown in Figure 6. The shapes of stress–strain curves of varying spinning speed indicate impacts of spinning speed on tensile properties. For the fiber SB0.7-1 (fiber produced with 0.7 g min^{-1} and 697 m min^{-1}) shows typical tensile deformation behavior of un-oriented fibers. It shows initial Hookean elastic deformation region, followed by the yield point and the plateau where the extension of fiber length with

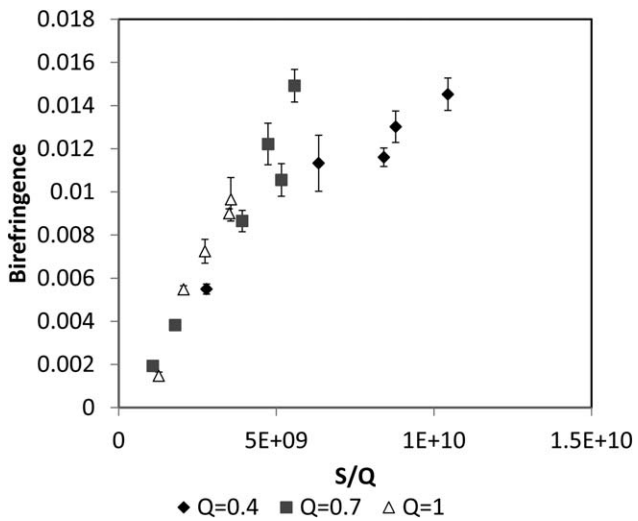

Figure 5. Birefringence of PLA fibers produced under various spinning conditions.

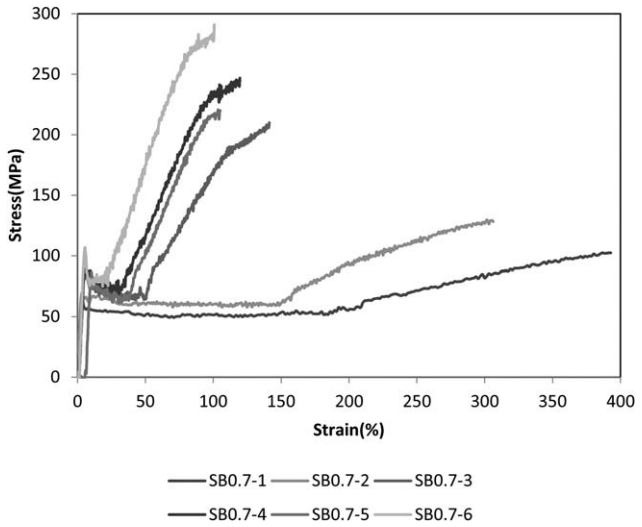

Figure 6. Typical Stress–strain curve of PLA filaments spun in spunbond line as the function of spinning speed. Throughput = 0.7 g min^{-1}.

little added force. Beyond this point, further elongation requires increasing tensile force and eventually fiber breakage occurs. As increases in spinning speed, the length of the plateau in SS curve getting shorter. We can also observe shift of breakages point to higher stress/lower strain region as expected. Effects of spinning speed on tensile properties are shown more clearly in Figure 7. Tensile modulus and breaking tensile strength increase with the spinning speed, while strain at break decreases. We can also see the effects of throughput (Figure 7). Decreasing throughput tends to increase tensile breaking strength, Young's modulus and decrease strain at break, even effects are not as strong as those of spinning speed.

The effects of spinning conditions—spinning speed and throughput on fiber tensile properties can be explained by differences in fiber fine structures developed during the spinning process. As discussed in previous sections, crystal formation and molecular orientation were improved by high spinning speed. It is well recognized that molecular orientation is a major governing factor of tensile deformation of fibers.[35] As shown in previous section, molecular orientation measured by birefringence is dependent on Q/S (throughput/spinning speed). Therefore, increasing fiber spinning speed and reduction of polymer throughput would lead to more oriented structure, which impact polymer tensile properties. The relationship between birefringence and breaking tensile strength and strain at break shown in Figure 8. Breaking tensile strength of PLA fibers in this study are almost linearly proportional to birefringence [Figure 8(a)]. So, increasing breaking tensile strength at high spinning speed can be attributed to enhanced molecular orientation. Strain at break [Figure 8(b)] also showed high dependency on birefringence and reduction of strain at break was observed in fibers with high molecular orientation.

What is more interesting is this trend holds for tensile properties of meltspun PLA filaments found in literatures (Figure 9).[10,12] When breaking tensile strength and strain at break of PLLA fibers are plotted against birefringence, all results more or less fall into a same line. Breaking tensile strength is linearly proportional to birefringence and strain at break is inversely proportional to birefringence even these three sets of data are produced by different spinning system and conditions. This indicates birefringence plays the crucial role in tensile properties of fibers regardless of spinning system used.

High dependence of tensile properties on molecular orientation can be explained by molecular orientation of spun fibers which

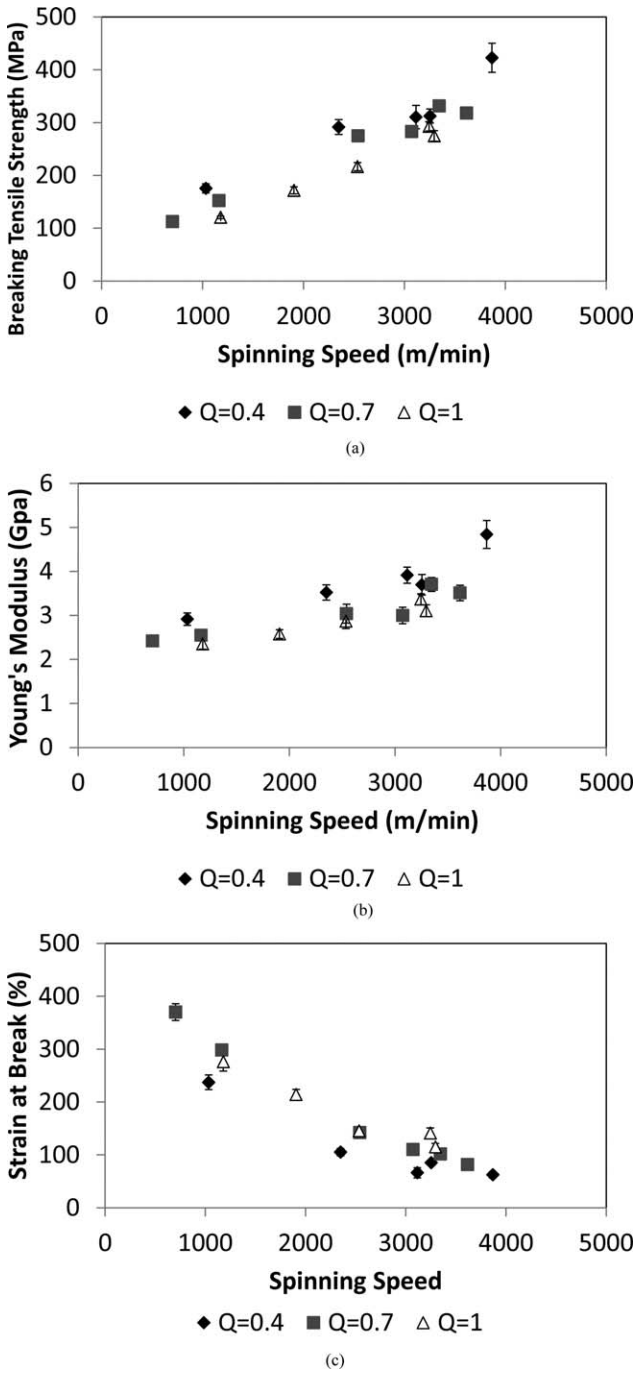

Figure 7. Effects of spinning conditions on single fiber tensile properties (a) Breaking tensile strength, (b) initial Young's modulus, and (c) strain at break.

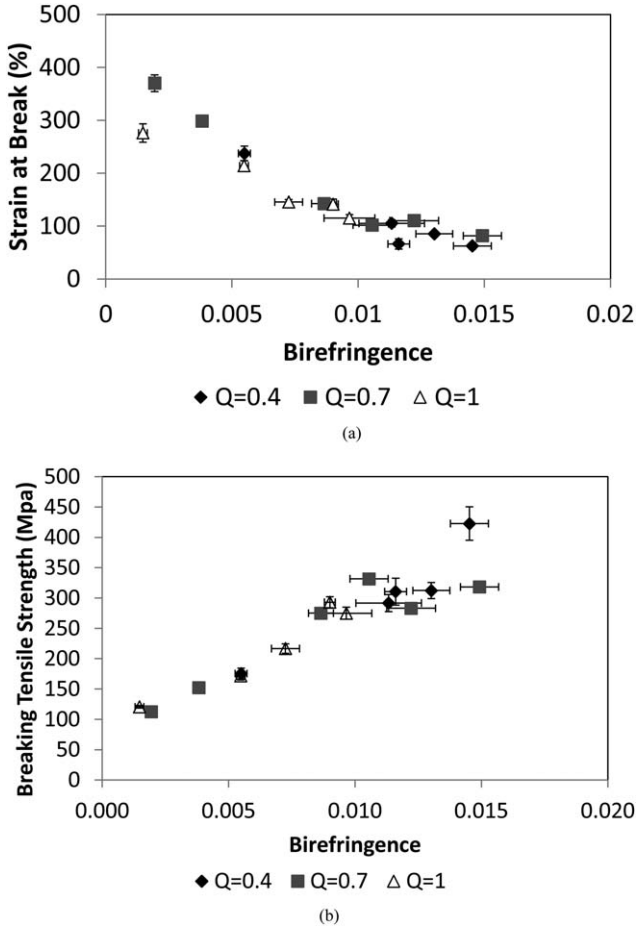

Figure 8. Effects of birefringence on single fiber tensile properties (a) Strain at break, and (b) breaking tensile strength.

are directly related to the length extension during the spinning process, as previously mentioned. If the length of a fiber with no molecular orientation is L_0 and the fiber is stretched to length L_s during the spinning process by spin-line tension, spun orientation of the spun fiber, *SO*, is simply ratio of two lengths because extension of fiber length is the results of realignment of molecules to fiber axis when no chain slippage occurs. Therefore, spun orientation becomes,

$$SO = \frac{L_S}{L_O} \tag{6}$$

Now, let us consider the force–elongation curve of the fiber with no molecular orientation (Figure 10). A fiber with initial length, L_0, will experience initial Hookean elastic deformation region to the yield point and the plateau where the extension of fiber length with little added force (open accompanied by macroscopic necking phenomena) to a specific length, known as natural draw length, L_n. Beyond this point, further elongation requires increasing tensile force and eventually fiber breakage occurs.

If no molecular orientation exist, natural draw length, L_n, length to break, L_B, and breaking force, F_B would be determined by polymer characteristics—molecular weight and chemical compositions. Therefore, L_B, F_B, and L_n can be considered as constants for a given polymer. Most fibers, however, almost always develop some degree of molecular orientation by the stretching of the fiber during spinning, so the length of fibers, L_S, with spun orientation, *SO*, will be larger than L_0. Then, the tensile force applied on a spun fiber, deformation curve (shown in Figure 10 as Fiber B) starts from L_S since it is already elongated to that point, and follow the same path to Fiber A (fiber with no orientation) and results in a reduction in elongation to break ($L_B - L_S$) and reduction in natural draw length (distance $L_N - L_S$), compared to a fiber with no orientation (elongation to breaks is L_B, natural draw length is L_n).

Strain at break, $E_B(\%)$, of the fiber with spun orientation, *SO* is defined as change of length at break point, which is

$$E_B(\%) = \frac{L_B - L_S}{L_S} \times 100 = \left(\frac{L_B/L_0}{L_S/L_0} - 1\right) \times 100 \tag{7}$$

We already assumed L_B (length at break) is constant, so

$$\frac{L_B}{L_0} = L^* = \text{constant} \tag{8}$$

Then,

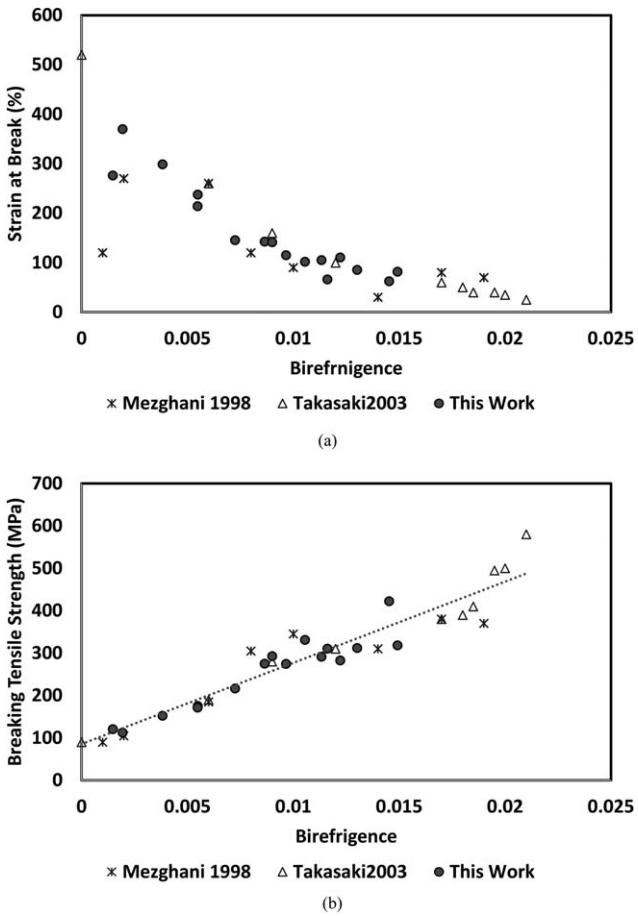

Figure 9. Comparison between fibers produced with spunbond system in this article and filaments fibers produced with textile melt spinning process reported at the literatures (a) strain at break and (b) breaking tensile strength.[10,12]

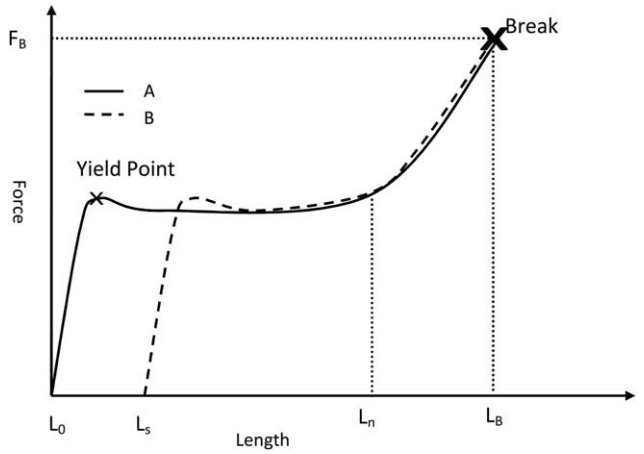

Figure 10. Force–elongation curve of the fiber. Fiber A: no molecular orientation, Fiber B: with a spun-orientation, SO.

$$\frac{E_B}{100} = \frac{L^*}{SO} - 1 \tag{9}$$

Then, *so* Strain at break is inversely proportional to molecular orientation, which agrees in Figure 8(a)

To explain the dependency of fiber tenacity, again consider a force–elongation curve of a fiber with no orientation and a spun fiber with initial length, L_S. Assume breaking force, F_B, length to break, L_B, and natural draw length L_n are constant. Breaking tensile strength (S_S) is breaking force per unit area,

$$S_S = \frac{F_B}{A_S} \tag{10}$$

while A_S is the cross-sectional area of a spun fiber.

Because of conservation of mass, elongation of fiber length to L_S leads to reduction of cross-sectional area. So,

$$\rho A_0 \cdot L_0 = \rho A_s \cdot L_s \tag{11}$$

while ρ is fiber density, A_0 is the cross-section area a fiber with no molecular orientation

Then,

$$S_s = \frac{F_b}{A_0} \cdot \frac{L_s}{L_0} = S_0 \cdot SO \tag{12}$$

Therefore, the tenacity of a fiber is linearly proportional to spun orientation [Figure 8(b)].

Natural Draw Ratio and Molecular Orientation

Total molecular orientation of fibers developed during the spinning governs tensile properties of fibers. However measurement of spun orientation is not always simple. It can be measured with an interference or a polarization microscope, but these are mostly limited to perfectly round and homogenous fibers. In addition, it is time consuming and complex method. In comparison, single fiber tensile property measurement is the more common and available and faster. Therefore, it would be valuable if one can estimate spun orientation of fibers using tensile properties. Arvidson *et al.*[36] suggested that once the relationship between birefringence and tensile behavior for a given polymer and the orientation can be estimated where the orientation cannot be directly measured.

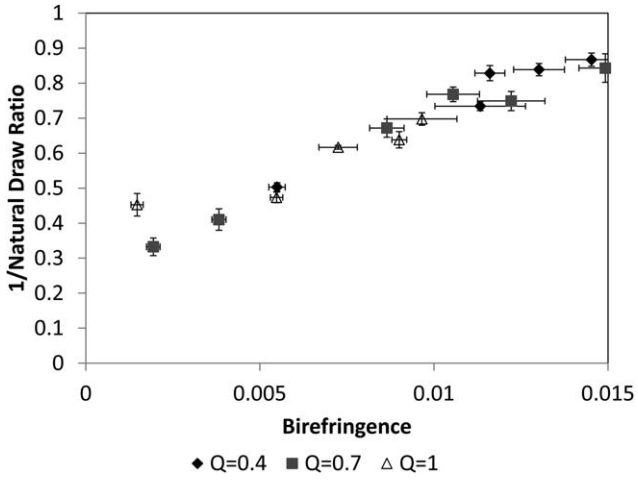

Figure 11. Relationship between molecular orientation and natural draw ratio.

To establish this relationship in PLA fibers, again we consider stress–strain curve of un-oriented fiber and spun fiber (Figure 10). The region of plateau where un-oriented molecules become

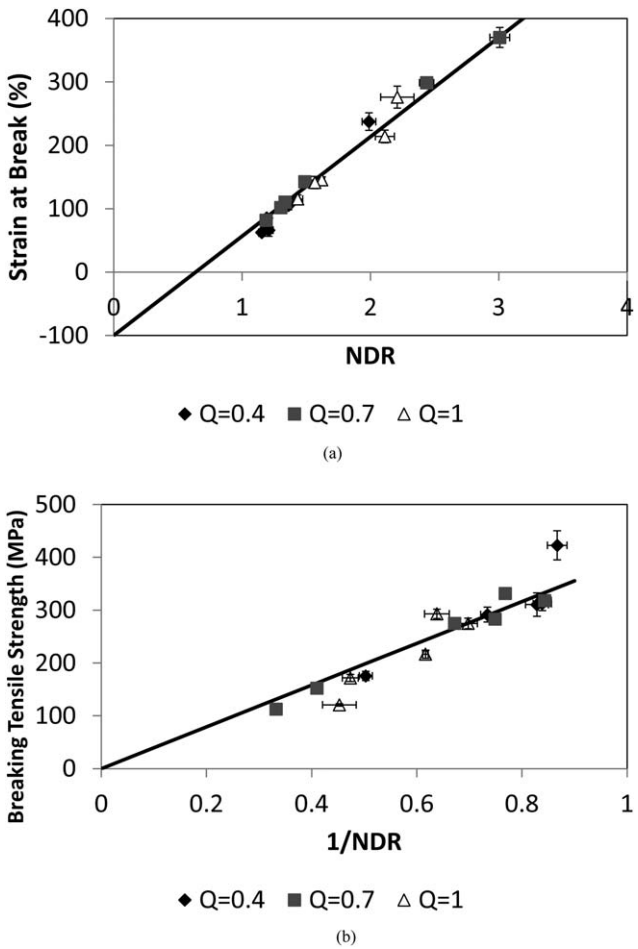

Figure 12. (a) Breaking tensile strength and (b) strain at break vs. Natural draw ratio.

oriented during the tensile deformation. So longer the plateau, less oriented fibers. We can evaluate length of this plateau by using natural draw ratio, which is the ratio of natural draw length to spun fiber length, L_s:

$$NDR = \frac{L_n}{L_s} \tag{13}$$

We already assumed L_n is a polymer constant, combining eqs. (6) and (13) yields,

$$NDR = \frac{L_n}{L_s} = \frac{L_n/L_0}{L_s/L_0} = \frac{K}{SO} \tag{14}$$

Therefore, natural draw ratio would be inversely proportional to spun orientation. This is in agreement with our experimental results illustrated in Figure 11. 1/NDR of PLA fibers and birefringence showed linear relationship regardless of its spinning speed and throughput.

Then, impact of *SO* (molecular orientation) on between tensile strength and tensile strain can be substituted with 1/*NDR* in eqs. (9) and (12).

For strain at break

$$E_B = \left(\frac{L^*}{SO} - 1\right) \cdot 100 = 100L^* \cdot NDR - 100 \tag{15}$$

For breaking tensile strength

$$S_s = \frac{F_b}{A_0} \cdot \frac{L_s}{L_0} = S_0 \cdot SO = \frac{T_0 K}{NDR} \tag{16}$$

Therefore, the tenacity of a fiber is inversely proportional to natural draw ratio. Figure 12(b) illustrates the relationship between *NDR* and tenacity of PLA filaments. Tenacity is linearly proportional to 1/*NDR* as expected in Eq. (16).

So we can conclude that *NDR* can be used as the measure of the spun orientation in the fibers and *SO* and *NDR* directly correlated to tensile properties including breaking tensile strength and strain at break.

CONCLUSIONS

Clearly, the melt spinning conditions of PLA fiber greatly influence the fiber structure developed. As spinning speed increases, crystallinity increases dramatically because of stress-induced crystallization as the result of increased spin line tension. Birefringence, which represent molecular orientation, was influenced by spinning speed and throughput. It was almost linear increase as *S*/*Q* increases. These changes in fiber structure influence fiber tensile properties. Breaking tensile, strain at break, initial modulus, and natural draw ratio were highly dependents on spinning condition. An increase in spinning speed leads to a higher breaking tensile strength, higher initial modulus, and lower strain at break. We have shown an almost linear relationship between breaking tensile strength of PLA fibers and birefringence indicating that improved tensile properties at high spinning speeds can be attributed to enhanced molecular orientation. The dependency of fiber tenacity and strain at break on spun orientation were explained with natural draw ratio as a measure of spun orientation.

REFERENCES

1. Drumright, R. E.; Gruber, P. R.; Henton, D. E. *Adv. Mater.* **2000**, *12*,
2. Mohanty, A. K.; Misra, M.; Drzal, L. T. Natural Fibers, Biopolymers and Biocomposites; CRC: Boca Raton, FL, **2005**.
3. Kale, G.; Auras, R.; Singh, S. P.; Narayan, R. *Polym. Test.* **2007**, *26*, 1049.
4. Shi, B.; Palfery, D. *J. Polym. Environ.* **2010**, *18*, 122.
5. Gruber, P. R.; Kolstad, J. J.; Hall, E. S.; Conn, R. S. E.; Ryan, C. M. United State Patent 5338822 (**1994**).
6. Nampoothiri, K. M.; Nair, N. R.; John, R. P. *Bioresour. Technol.* **2010**, *101*, 8493.
7. Avine, O.; Khoddami, A. *Fibre Chem.* **2009**, *41*, 391.
8. Dugan, J. *Int. Nonwovens J.* **2001**, *10*, 29.
9. Fambri, L.; Pegoretti, A.; Fenner, R.; Incardona, S. D.; Migliaseri, C. *Polymer* **1997**, *38*, 79.
10. Mezghani, K.; Spruiell, J. E. *J. Polym. Sci. Part B: Polym. Phys.* **1998**, *36*, 1005.
11. Cicero, J.; Dorgan, J. R. *J. Polym. Environ.* **2001**, *9*, 1.
12. Takasaki, M.; Ito, H.; Kikutani, T. *J. Macromol. Sci. Part B: Phys.* **2003**, *B42*, 57.
13. Takasaki, M.; Ito, H.; Kikutani, T. *J. Macromol. Sci. Part B: Phys.* **2003**, *B42*, 403.
14. Schmack, G.; Tandler, B.; Optiz, G.; Vogel, R.; Komber, H.; Häußler, L.; Voigt, D.; Weinmann, S.; Heinemann, M.; Fritz, H. G. *J. Appl. Polym. Sci.* **2004**, *91*, 800.
15. Eling, B.; Gogolewski, S.; Pennings, A. *Polymer* **1982**, *23*, 1587.
16. Leenslag, J. W.; Pennings, A. *J. Polymer* **1987**, *28*, 1695.
17. Gupta, B.; Revagade, N.; Anjum, N.; Atthoff, B.; Hilborn, J. *J. Appl. Polym. Sci.* **2006**, *101*, 3774.
18. Horacek, I.; Kalisek, V. *J. Appl. Polym. Sci.* **1994**, *54*, 1751.
19. Honarbakhsh, S.; Pourdeyhimi, B. *J. Mater. Sci.* **2011**, *46*, 2874.
20. Zhou, H.; Green, T. B.; Joo, Y. L. *Polymer* **2006**, *47*, 7497.
21. Smyth, M.; Poursorkhabi, V.; Mohanty, A. K.; Gregori, S.; Misra, M. *J. Mater. Sci.* **2014**, *49*, 2430.
22. Schneider, A K. Unite State Patent 3636956 (**1972**).
23. Bansal, V.; Shambaugh, R. L. *Polym. Eng. Sci.* **1998**, *38*, 1959.,
24. Schmack, G.; Tandler, B.; Vogel, R.; Beyreuther, R.; Jacobsen, S.; Fritz, H. *J. Appl. Polym. Sci.* **1999**, *73*, 2785.
25. Batra, S.; Pourdeyhimi, B. Introduction to Nonwoven Technology; DEStech Publications: Lancaster, p **2012**.
26. Gruber, P. R.; Kolstad, J. J.; Ryan, C. M.; Conn, R. S. E.; Hall, E. S. United State Patent 6111060 (**2000**).
27. Persson, M.; Cho, S. -W.; Skrifvars, M. *J. Mater. Sci.* **2013**, *48*, 3055.
28. Bruckmoser, K.; Resch, K. *J. Appl. Polym. Sci.* **2015**, *132*, DOI: 10.1002/app.42432.

29. Arvidson, S. A.; Wong, K. C.; Gorga, R. E.; Khan, S. A. *Polymer* **2012**, *53*, 791.
30. Park, S. D.; Todo, M.; Arakawa, K. *J. Mater. Sci.* **2004**, *39*, 1113.
31. Gupta, B.; Revagade, N.; Hilbron, J. *Prog. Polym. Sci.* **2007**, *32*, 455.
32. Solarski, S.; Ferreira, M.; Devaux, E. *Polymer* **2005**, *46*, 11187.
33. Heuvel, H. M.; Huisman, R. *J. Appl. Polym. Sci.* **1978**, *22*, 2229.
34. Bosely, D. E. *J. Polym. Sci. C* **1967**, *20*, 77.
35. Morton, W. E.; Hearle, J. W. S. Physical Properties of Textiles Fibers, 4th ed.; Woodhead Publishing: Cambridge England, **2008**; p 301.
36. Arvidson, S. A.; Khan, S. A.; Gorga, R. E. *Macromolecules* **2010**, *43*, 2916.